

# Application of the orthotropic Rankine-type model to masonry panels

P. Bilko<sup>1</sup>, L. Malyszko<sup>2</sup>

<sup>1</sup>Faculty of Technical Sciences, University of Warmia and Mazury in Olsztyn, POLAND

**ABSTRACT:** The second author presented the orthotropic Rankine-type plasticity model for the analysis of structural problems in the plane stress state during the previous local seminar of IASS PC in Warsaw. The model included a maximum principal stress failure criterion of Rankine both for tension and compression regimes by incorporating the second order strength tensor. Within the framework of the finite element method for the elastoplasticity theory of small strains for softening/hardening materials, two yield surfaces resulting from the orthotropic principal stress criterion were implemented at the integration point level into the proprietary finite element program by means of user-defined subroutines. This paper demonstrates an application of the model to the analysis of a masonry panel. The numerical tests have been done in order to check the possibility of the model to reproduce an orthotropic behaviour of masonry panels with different tensile and compressive strengths along the material axes as well as different inelastic behaviour for each material axis after the own numerical implementation in the finite element code. The ability of the model to reproduce a failure mode of the panels is also of interest.

**Key words:** masonry, orthotropic failure criteria, rate-independent softening plasticity, numerical implementation, finite element method

## 1. INTRODUCTION

A large number of buildings, including these that may correspond with the lightweight structure definition, are constructed with masonry infill walls for architectural needs or the fire rating and sound transmission reasons. The walls can also greatly stiffen a flexible steel or reinforced concrete frame and significantly affect the distribution of lateral loads to various parts of the building. However, unreinforced masonry may be assumed a homogeneous but obviously anisotropic material, which exhibits distinct directional properties due to the influence of the mortar joints acting as planes of weakness. A model must reproduce an orthotropic material with different tensile and compressive strengths along the material axes as well as different inelastic behaviour for each material axis. A reduced number of orthotropic material models that may be specific for masonry have been proposed. An attempt of formulating one of them is the orthotropic Rankine-type model proposed by Malyszko (Ref 4). The model was presented during previous PC IASS seminar in Warsaw. This paper continues the previous work and illustrates behaviour of the masonry panels regarded as equivalent orthotropic continuum under a directional loading. Masonry is an example of a material for which the model applies, having different strengths parallel and perpendicular to the bed joints. The possibility of formulating robust numerical algorithms by means of user-defined subroutines of the proprietary nonlinear finite element program is also of prime importance. The constitutive model for the plane stress is provided with the framework of the mathematical elastoplasticity theory of small strains for softening materials. Here, the model for compression regime is a novel development. The implementation of the model is done within a framework of an incremental-iterative algorithm of finite element method using both the return-mapping algorithm allowing the stresses to be returned to the yield surface and a consistent tangent stiffness operator. The paper is concluded by presenting some numerical results of a masonry panel analysis verifying own implementation.

## 2. ORTHOTROPIC RANKINE-TYPE PLASTICITY MODEL

For the sake of simplicity, the mechanical description of the elastic-plastic model is presented in a state of plane stress parallel to the  $XZ$ -plane based on the assumption that the principal axes of orthotropy coincided with the frame of reference. The constitutive relation between stresses  $\boldsymbol{\sigma} = (\sigma_x, \sigma_z, \tau_{xz})$  and strains  $\boldsymbol{\varepsilon} = (\varepsilon_x, \varepsilon_z, \gamma_{xz})$  are given in a material point. Within the framework of the theory of elastoplasticity, the orthotropic Rankine-type failure criteria (2) and (4) serve as the yield surfaces and have to distinguish between domains of the different material response by means of the yield condition given by the yield sur-

face  $f$ . Within the yield surface ( $f < 0$ ), the material behaves elastically. On the yield surface ( $f = 0$ ), the material begins to yield. Thus, in the phenomenological approach that is applied in the present model, the geometrical nonlinearity like cracking is accounted for by the introduction of a loading function  $f$  describing the failure criterion. By the assumption of small strains, the function  $f$  is set up with quantities that refer to the undeformed configuration.

### 2.1. Orthotropic failure criteria

In an arbitrary right-handed Cartesian coordinate system  $\{x_i\}$  coaxial with the axes of the principal stresses and for a so-called generalized plane state problem when  $\sigma_2$  is equal to zero, the failure criterion for the tension regime can be written in the following form

$$\left( \frac{\cos^2 \alpha}{f_{tX}} + \frac{\sin^2 \alpha}{f_{tZ}} \right) \sigma_1 - \frac{\sigma_1 \sigma_3}{f_{tX} f_{tZ}} + \left( \frac{\cos^2 \alpha}{f_{tZ}} + \frac{\sin^2 \alpha}{f_{tX}} \right) \sigma_3 = 1 \quad (1)$$

where the angle  $\alpha$  in the direction cosines measures the rotation between the first axis  $x_1$ , i.e. the axis of the first principal stress  $\sigma_1$  and the first material X-axis. The parameters  $f_{tX}$  and  $f_{tZ}$  denote the tensile strengths that may be determined from the simple tension tests along the direction of the material axes. In the  $\{x_i\}$  frame coaxial with the  $XZ$  axes, where  $X$  and  $Z$  are the principal axes of material orthotropy, the failure criterion can be written as

$$(f_{tX} - \sigma_x)(f_{tZ} - \sigma_z) - \tau_{xz}^2 = 0 \quad (2)$$

For the compression regime, the similar form of the failure criterion can be obtained by replacing the tensile strengths by the compressive strengths with positive values, i.e. by the strengths  $-f_{cX}$  and  $-f_{cZ}$ . The failure condition caused by the compression can be written as

$$\left( \frac{\cos^2 \alpha}{f_{cX}} + \frac{\sin^2 \alpha}{f_{cZ}} \right) \sigma_1 + \frac{\sigma_1 \sigma_3}{f_{cX} f_{cZ}} + \left( \frac{\cos^2 \alpha}{f_{cZ}} + \frac{\sin^2 \alpha}{f_{cX}} \right) \sigma_3 = -1 \quad (3)$$

instead of Eqn (1) and as

$$(f_{cX} + \sigma_x)(f_{cZ} + \sigma_z) - \tau_{xz}^2 = 0 \quad (4)$$

instead of Eqn (2).

As one can see, a representation of an orthotropic failure surface in term of principal stresses only is not possible. For plane stress situation, a

graphical representation can be obtained either in terms of the full stress vector ( $\sigma_x, \sigma_z$  and  $\tau_{xz}$ ), referred to the material axes, or in terms of principal stresses and the angle  $\alpha$ . It is obvious that it is not possible to formulate the failure criterion of orthotropic material in terms of the principal stresses only, since they are isotropic functions of the stress state. In Fig. 1, a comparison of the proposed criteria with experimental data of masonry specimens subjected to biaxial tests are presented. The material parameters are taken from Page (Refs 8, 9). The comparison shows quite good agreement in the tensile regime, less good agreement in compressive regime and a discrepancy in the shear regime. Some improvements are needed which may be done either by an introduction of a correction factor in the Rankine criterion or by addition a third criterion specified for the shear failure. The former method is presented in Ref 4. In Refs (5, 6) Malyszko discusses the latter method within simplified forms of the failure criterion.

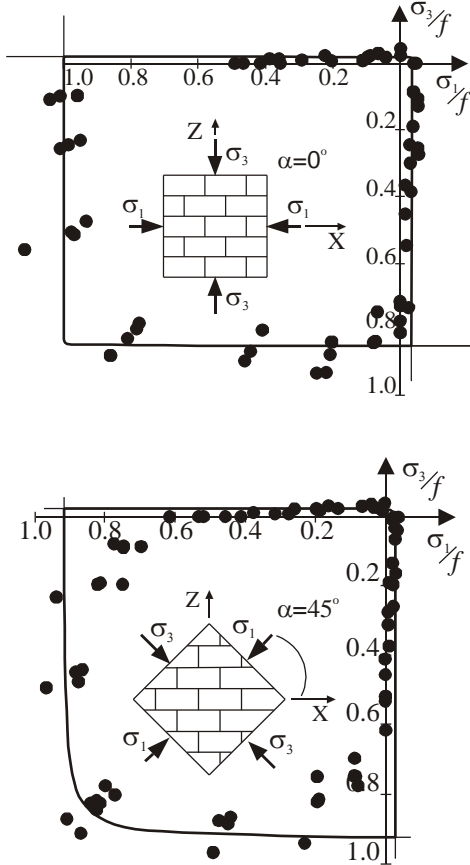


Fig.1. Contours of generalized failure criterion of Rankine for strength parameters:  $f_{tX}=0.3, f_{tZ}=0.15, f_{cX}=10.0, f_{cZ}=8.5$  [MPa] with comparison with experimental data from Page (Refs 8, 9)

## 2.2. Elastic-plastic constitutive model

Within the framework of the theory of elastoplasticity, the orthotropic Rankine-type criteria (2) and (4) serve as the yield surfaces. They have to distinguish between domains of the elastic and plastic material response in the tension and the compression regimes by the introduction of loading functions  $f_\beta$  of the stress  $\sigma$  and the internal state parameter  $\kappa_\beta$ , where  $\beta=t$  for tension and  $\beta=c$  for compression regime. Within the yield surface ( $f_\beta < 0$ ), the material behaves elastically according to the linear Hooke's law

$$\sigma = \mathbf{D}\boldsymbol{\varepsilon}^{el} = \mathbf{D}(\boldsymbol{\varepsilon} - \boldsymbol{\varepsilon}^{pl}) \quad (5)$$

where in accordance with the usual approach of the flow theory of plasticity, the basic assumption of additive strain decomposition of the strain tensor  $\boldsymbol{\varepsilon}$  into an elastic part  $\boldsymbol{\varepsilon}^{el}$  and an irreversible plastic part  $\boldsymbol{\varepsilon}^{pl}$  is made. For an orthotropic or transversely isotropic material in a so-called generalized plane stress problem in the  $XZ$ -plane, the elastic parameters are represented by the matrix  $\mathbf{D}$  that contains four material constants: two Young's moduli  $E_x$  and  $E_z$ , one shear module  $G_{xz}$  and Poisson's ratio  $\nu$ .

On the yield surface ( $f_\beta = 0$ ), the material begins to yield. The inelastic strain  $\boldsymbol{\varepsilon}^{pl}$  may be nonzero. The inelastic strain rate in the intersection of the different yield surfaces is obtained from a linear combination of the plastic strain rate of the tensile and compressive yield surfaces according to Koiter's generalization

$$\dot{\boldsymbol{\varepsilon}}^{pl} = \dot{\boldsymbol{\varepsilon}}_t^{pl} + \dot{\boldsymbol{\varepsilon}}_c^{pl} = \dot{\lambda}_t \frac{\partial g_t}{\partial \boldsymbol{\sigma}} + \dot{\lambda}_c \frac{\partial g_c}{\partial \boldsymbol{\sigma}} \quad (6)$$

where  $\dot{\lambda}_t, \dot{\lambda}_c$  are inelastic multipliers and  $g_t, g_c$  are plastic potentials in tension and compression regimes, respectively.

The inelastic behaviour can be described by a strain softening hypothesis given by the maximum and minimum principal plastic strains in tension and compression regime, respectively. Thus, the particularly simple expression  $\dot{\kappa}_\beta = \dot{\lambda}_\beta$  may be recovered for the internal state parameters  $\kappa_\beta$ .

## 2.3. Implementation in a finite element code

The model has been coded in Fortran programming language (Ref 1) and next implemented in a proprietary finite element code *Diana* using the user-supplied subroutine *usrmat* (Ref 2). The subroutine lets the user specify a general nonlinear material behaviour by updating the state variables over the equilibrium step  $n \rightarrow n+1$  in the iterative local Newton-Raphson procedure. The implicit Euler backward algorithm is used. Assuming that the tension and compression regimes are uncoupled, in the presence of plastic flow, the return mapping algorithm for the corner regime reduces to the following system of five nonlinear equations containing five unknowns (the  $\boldsymbol{\sigma}_{n+1}$  components,  $\Delta\kappa_{t,n+1} = \Delta\lambda_{t,n+1}$  and  $\Delta\kappa_{c,n+1} = \Delta\lambda_{c,n+1}$ )

$$\left\{ \begin{array}{l} \mathbf{D}^{-1}(\boldsymbol{\sigma}_{n+1} - \boldsymbol{\sigma}^{trial}) + \Delta\lambda_{t,n+1} \frac{\partial g_t}{\partial \boldsymbol{\sigma}}|_{n+1} + \Delta\lambda_{c,n+1} \frac{\partial g_c}{\partial \boldsymbol{\sigma}}|_{n+1} = \mathbf{0} \\ f_{t,n+1} = \sqrt{\frac{1}{2} \boldsymbol{\xi}_{t,n+1}^T \mathbf{P} \boldsymbol{\xi}_{t,n+1}} + \frac{1}{2} \boldsymbol{\xi}_{t,n+1}^T \boldsymbol{\pi} = 0 \\ f_{c,n+1} = \sqrt{\frac{1}{2} \boldsymbol{\xi}_{c,n+1}^T \mathbf{P} \boldsymbol{\xi}_{c,n+1}} - \frac{1}{2} \boldsymbol{\xi}_{c,n+1}^T \boldsymbol{\pi} = 0 \end{array} \right. \quad (7)$$

where the trial stress is

$$\boldsymbol{\sigma}^{trial} = \boldsymbol{\sigma}_n + \mathbf{D} \Delta \boldsymbol{\varepsilon}_{n+1} \quad (8)$$

and (Eqn 9)

$$\mathbf{P}_\beta = \frac{1}{2} \begin{bmatrix} 1 & -1 & 0 \\ -1 & 1 & 0 \\ 0 & 0 & 4\gamma_\beta \end{bmatrix}, \boldsymbol{\pi} = \begin{bmatrix} 1 \\ 1 \\ 0 \end{bmatrix}, \boldsymbol{\xi}_\beta = \boldsymbol{\sigma} - \boldsymbol{\eta}_\beta, \boldsymbol{\eta}_t = \begin{bmatrix} \tilde{f}_{tX} \\ \tilde{f}_{tZ} \\ 0 \end{bmatrix}, \boldsymbol{\eta}_c = - \begin{bmatrix} \tilde{f}_{cX} \\ \tilde{f}_{cZ} \\ 0 \end{bmatrix}$$

Note that Eqns (2, 4) are recast in a matrix form in Eqns. (7,4,5). Also, the additional parameters  $\gamma_\beta$  are introduced in the projection matrix  $\mathbf{P}$  in Eqn (9) in order to control the shear stress contribution to failure instead of  $\gamma_\beta = 1.0$  being the standard Rankine value. If the standard values are used in failure criteria, the model can underestimate the shear-compression part in terms of biaxial loading. However, the failure criteria (7,4,5) with the standard value may be taken as the plastic potentials  $g$ . If the projection matrix  $\mathbf{P}$  with the standard value  $\gamma_\beta = 1.0$  is taken in the plastic potentials  $g$  and, at the same time, the value  $\gamma_\beta \neq 1$  is taken in the yield criteria (7,4,5) then the non-associated flow rule is applied, both for tension and compression regimes. The value  $\gamma_\beta$  may be determined as

$$\gamma_\beta = f_{\beta X0} f_{\beta Z0} / \tau_\beta^2 \quad (10)$$

where  $\tau_\beta$  are the pure shear strengths in tension and compression, respectively. The values  $f_{\beta X0}$  and  $f_{\beta Z0}$  are the characteristic yield values (initial or peak) of the uniaxial strengths in the direction of the material  $X, Z$  axes that may be obtained from appropriate equivalent stress-equivalent strain softening/hardening diagrams  $\tilde{f}_{\beta X}(\kappa_\beta), \tilde{f}_{\beta Z}(\kappa_\beta)$ , with different fracture energies  $G_{\beta X}, G_{\beta Z}$  for each yield value, see Ref 4 for details. Note that in Eqn (9) two additional strength parameters are introduced ( $\gamma_t$  and  $\gamma_c$ ).

For the testing of the directional mechanical response of the model with *Diana* a single-element test was chosen under displacement control, with

dimensions  $100 \times 100 \text{ [mm}^2\text{]}$  (Fig. 2). The elastic material parameters are  $E_x=7500 \text{ MPa}$ ,  $E_z=4000 \text{ MPa}$ ,  $\nu=0,15$  and  $G_{xz}=1400 \text{ MPa}$ .

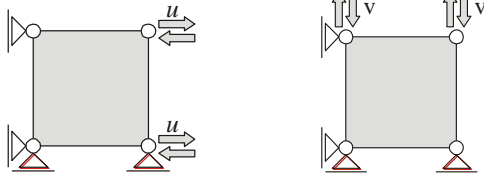


Fig. 2. Uniaxial tension and compression problem: a) loading in horizontal direction, b) loading in vertical direction

The inelastic material parameters are given in Tab. 1. The additional material parameter, the equivalent plastic strain  $\kappa_{cp}$  corresponding to the peak compressive strength according to softening/hardening law, equals to 0.002. The equivalent length used to regularize the results with the respect to mesh refinement, is equal to  $0.1 \text{ m}$ .

Table 1. Inelastic material parameters

Tension regime				Compression regime				Both
$f_{ix}$	$f_{iz}$	$G_{ix}$	$G_{iz}$	$f_{cx}$	$f_{cz}$	$G_{cx}$	$G_{cz}$	$\gamma \beta$
MPa	MPa	$\frac{\text{kNm}}{\text{m}^2}$	$\frac{\text{kNm}}{\text{m}^2}$	MPa	MPa	$\frac{\text{kNm}}{\text{m}^2}$	$\frac{\text{kNm}}{\text{m}^2}$	
0.35	0.25	0.05	0.015	10.0	8.8	20.0	15.0	1.0

#### Uniaxial problem - loading in the horizontal direction.

Figure 3 (top) shows the stress-strain response for the tensile loading along the horizontal X-axis (along the masonry bed joints). When the tensile stress equals to  $0.35 \text{ MPa}$  is reached, the material strength degrades according to the exponential tensile softening of the theoretical model. The anticipated constitutive behaviour is exactly reproduced. The stress-strain response for the compressive loading along the same direction is shown at the bottom of the Fig. 3. Again, when the compressive stress equals to  $10 \text{ MPa}$  is reached, the material strength degrades according to the hardening/softening law with a residual plateau from the theoretical model.

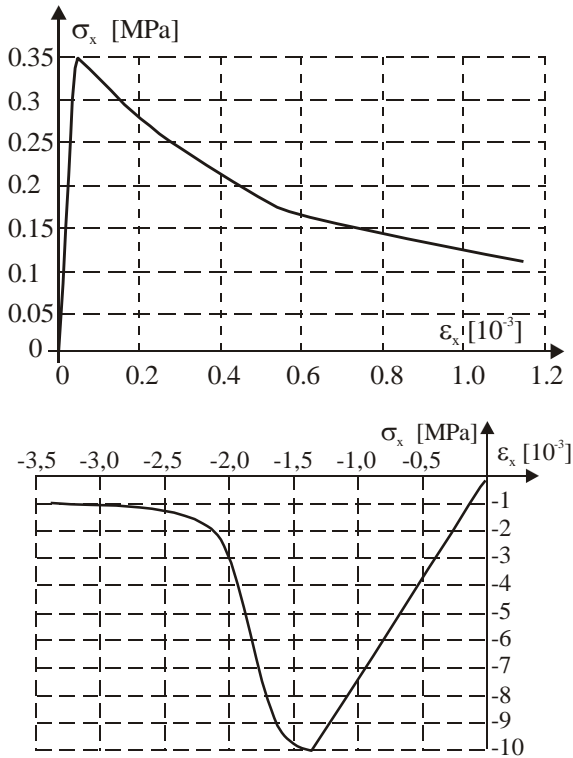


Fig. 3. Stress-strain response in horizontal tension and compression

#### Uniaxial problem - loading in the vertical direction.

The stress-strain response for the tensile loading along the vertical Z-axis (perpendicular to the masonry bed joints) is shown at the top of Fig. 4. Now the material strength degrades according to the exponential tensile softening of the theoretical model when the tensile stress equals to  $0.25 \text{ MPa}$ . The bottom of the Fig. 4 shows the stress-strain response for the compressive loading along the same direction. Again, when the compressive strength equal now to  $8.8 \text{ MPa}$  is reached, the material strength degrades according to the hardening/softening law with a similar residual plateau as in loading in horizontal direction.

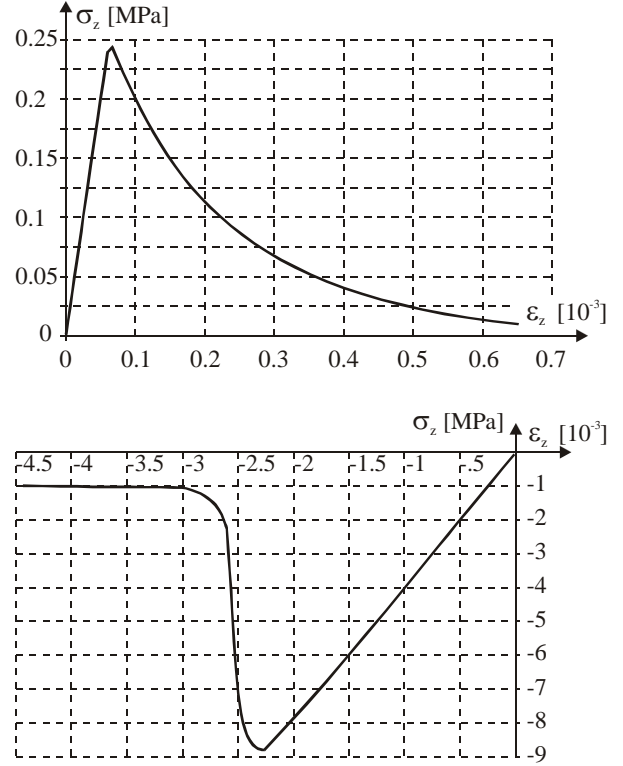


Fig. 4. Stress-strain response in vertical tension and compression

**The shear model problem** is a single element test for disclosing the basic behaviour of the constitutive model in shearing. The test loads an element as shown in Fig. 5. The displacements in the vertical direction are constrained. Because of symmetry of the failure contours relative to hydrostatic axis the similar test with vertical loading will give similar results, thus the test in Fig. 5 is the only one considered. Figure 6 shows

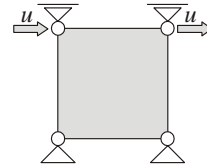


Fig. 5. Shear model problem

the stress-strain response in terms of the shear components. In this test, the tensile yield surface is active. For the value of the parameter  $\gamma_t$  equal to 1.0, the shear failure stress is

$$\tau_f = \sqrt{f_{ix} f_{iz}} \quad (11)$$

which means that for the strength parameters given in Tab. 1  $\tau_f = 0.30 \text{ MPa}$  as one can see in Fig. 6. When the shear stress reaches the value of  $0.3 \text{ MPa}$  shear strength degrades in similar manner as the tensile strengths do.

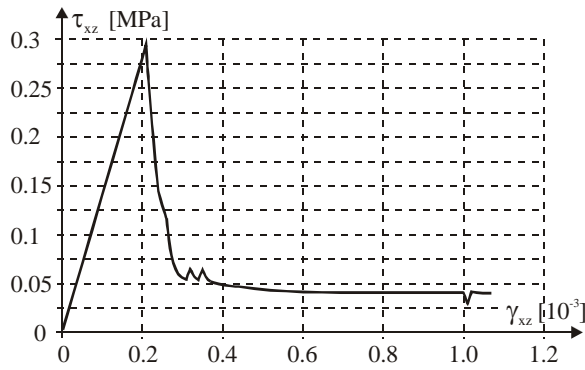


Fig. 6. Shear stress-strain response in single element test

### 3. APPLICATION TO THE ANALYSIS OF MASONRY PANEL

The only example analysed is a masonry shear wall, 1 m square, without an opening built of 18 courses of masonry, from which the top and bottom courses are fully clamped in steel beams. An initial vertical load equals to  $0.30 \text{ MPa}$  is applied before shearing the wall with the horizontal force  $F$ . The top edge remains elastic constrained and can move a little upwards upon shearing with a horizontal displacement  $\delta$ , see Fig. 7.

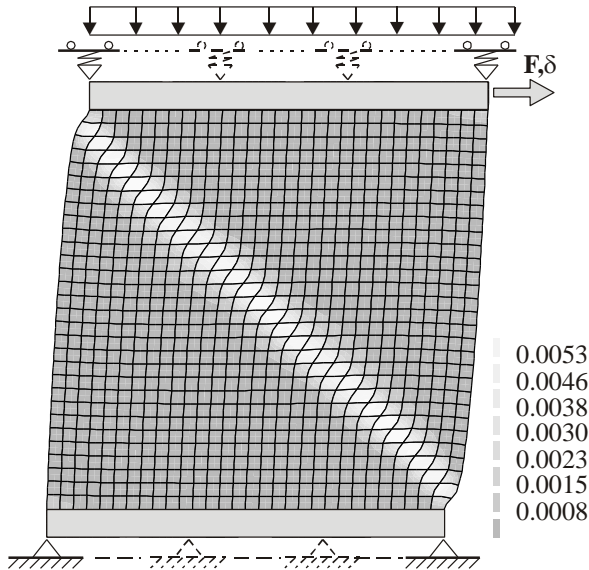


Fig. 7. Masonry shear wall. Maximum principal strain for  $\delta=9 \text{ mm}$

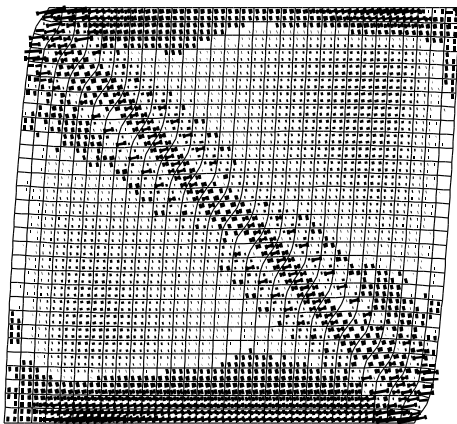


Fig. 8. Masonry shear wall. Maximum principal stress for  $\delta=9 \text{ mm}$

The inelastic material parameters are given in Tab.1 and the elastic parameters in Tab. 2. Figure 8 shows the results of the analysis in a vector form of the maximum principal stress for the horizontal displacement  $\delta=9 \text{ mm}$  at the time when the diagonal crack starts forming. As expected

Tab.2. Elastic material parameters of masonry shear wall

$E_x$	$E_z$	$\nu_{xz}$	$G_{xz}$
7520 MPa	3960 MPa	0.09	1460 MPa

in most cases of unconfined masonry structures, the failure mechanism is determined by tensile behaviour. However, due to some difficulties in the analysis after the own implementation, the failure mode is slightly different from that obtained in Ref 3.

### 4. FINAL REMARKS

Although the tension softening and compression hardening/softening that may capture the total degradation process are taken into account in the model, some improvements have to be done by addition a third criterion specified for the shear failure. It seems that the generalization of the Coulomb-Mohr failure criterion combined with Rankine-type criterion should be included in the model, see Ref 7. The addition of this criterion should help controlling the shear stress contribution to the failure and proper estimate shear-compression and shear-tension regimes of the model. Due to the large number of material parameters, involved in the model, analyses have to be carried out in different structures to assess the influence of the variation of the material parameters on the structural response of the masonry panels.

### 5. REFERENCES

1. COMPAQ Visual Fortran Version 6.6. Professional Edition 2001. *Compaq Fortran Language Reference Manual*. Compaq Computer Corporation.
2. DIANA – Finite Element Analysis. 2002. *User's Manual*. Release 8.1. Vol. 1 - 9, Published by: TNO Building and Construction Research, The Netherlands.
3. P.B. Lourenco: *Two aspects related to the analysis of masonry structures: Size effect and parameter sensibility*. TUDelft, Faculty of Civil Engineering and Geosciences, Mechanics & Structures, Computational Mechanics, Report 03.21.1.31.25, December 1997
4. L. Małyszko: *Orthotropic Rankine-type plasticity model*. Proceedings of the International Colloquium of IASS Polish Chapter on Lightweight Structures in Civil Engineering, 12-14 September, 2005, p. 286-293.
5. L. Małyszko: *Failure Criteria for Masonry as Anisotropic Material*. Proceedings of the 4<sup>th</sup> Intern. Conf. "Analytical Models and New Concepts in Concrete and Masonry Structures", 5-8 June, Cracow 2002, p. 111-115.
6. L. Małyszko: *The Rankine-type criterion aimed at describing masonry orthotropy*. Proceedings of Structural Analysis of Historical Constructions, New Delhi 2006, P.B. Lourenço, P. Roca, C. Modena, S. Agrawal (Eds.), ISBN 972-8692-27-7.
7. L. Małyszko: *Failure modelling in masonry structures taking into account anisotropy*. Wydawnictwo UWM, Olsztyn 2005. (in Polish)
8. W. Page: *The biaxial compressive strength of brick masonry*. *Proc. Int. Civ. Engrs, Part 2*, 71, 1981, p. 893-906.
9. W. Page: *The strength of brick masonry under biaxial compression*. *Int.J. Masonry Constr.*, 3(1), 1983, p.26-31.

<sup>1</sup>Piotr Bilko, Department of Geotechnology and Structural Mechanics, ul. Prawocheńskiego 19, 10-900 Olsztyn, Poland, e-mail: bilko-piotr@o2.pl

<sup>2</sup>Leszek Małyszko, Department of Geotechnology and Structural Mechanics, e-mail: leszek.malyszko@uwm.edu.pl